The Distortion of a Baroclinic Fofonoff Gyre by Wind Forcing

A. J. GEORGE NURSER

Space and Atmospheric Physics Group, Department of Physics, Imperial College, London

(Manuscript received 25 February 1987, in final form 18 August 1987)

ABSTRACT

The subtropical recirculation regions are considered as examples of nonlinear free flow—"baroclinic Fofonoff gyres." In the interior, where relative vorticity may be neglected, the quasi-geostrophic assumption may be relaxed, and the layered treatment extended to a continuously stratified model. The implied density field is compared with observations.

The deformation of the inertial gyre caused by the presence of an anticyclonic wind stress curl is then considered. In addition to the recirculating "free" component of the flow along latitude circles, there is a meridional component whose depth-integrated transport is set by the magnitude of the imposed wind stress curl. It is found that the "bowl" within which the recirculation is contained deepens towards the north and west, and exhibits the "champagne glass" structure found in the quasi-geostrophic eddy-resolving numerical models.

1. Introduction

Examination of the flow patterns in the region of separation of the western boundary current (WBC), both in numerical models [Fig. 1, from the quasi-geostrophic n-level model of Holland (Holland et al. 1984)] and in the observations (Fig. 2, Worthington's, 1976, scheme for mass transport in the northwest Atlantic), makes apparent the deficiencies of the classical frictional boundary layer–Sverdrup balance models of Munk (1950) and Stommel (1948) as paradigms of the circulation.

Rather than returning to the interior from a gradually shrinking WBC, as prescribed by these linear models, the fluid leaves the coast in a definite jet. A considerable proportion of this outflow becomes trapped in an anticyclonic recirculation which pumps the fluid back into the WBC. The circulation is thus "overspun"; the maximum transport carried by the WBC is much greater than the maximum southward Sverdrup transport. In the Atlantic, it is estimated that circa 200 Sv (Sv $\equiv 10^6$ m^3 s^{-1}) flows in the Gulf Stream off Cape Hatteras (Hogg, 1983; Richardson, 1985) compared to the Sverdrup transport of only 30 Sv across 30°N (Wunsch and Roemmich, 1985; Leetmaa and Bunker, 1977).

This difference between the observed circulation and the predictions from the linear models is paralleled by differing diagnoses of the equilibrative processes. In the classical models, the anticyclonic vorticity imparted to the fluid by the wind stress curl is eroded by friction in the WBC. However, evidence from high resolution eddy resolving models (Marshall, 1984) suggests that vorticity transfer by eddies across the separated Gulf Stream is likely to make an important contribution to the vorticity budget of the gyre.

It is, therefore, suggested (Marshall and Nurser, 1986; henceforth MN) that there may be some merit in considering a baroclinic generalization (Fofonoff, 1962; MN) of the Fofonoff gyre as a paradigm for the flow in the recirculation region. This features (see Fig. 3) a narrow eastward jet modeling the separated Gulf Stream, with broad westward return flow south of the jet becoming more restricted towards the axis of the stream with increasing depth. Such a gyre is a "free mode": the meridional displacement of the fluid in the WBC is made possible by conversion of planetary vorticity into vortex stretching and relative vorticity in such a manner as to conserve potential vorticity. This contrasts with the classical linear theory in which potential vorticity is created or destroyed directly by forcing and dissipation.

Clearly, forcing and dissipation *do* play a role; in the model presented here, the transport (and changes in potential vorticity) driven directly by the forcing and dissipation are supposed to be "small" compared with the free component of the flow (and interconversions between the various manifestations of the potential vorticity). Rather than starting from an ocean which is almost everywhere Sverdrupian, and allowing a small degree of "inertiality," as, for example, in the analytical model of Veronis (1966), we take an ocean in "free flow" as the starting point and consider the distortion of this free flow consequent upon wind stress curl forcing and dissipation.

Corresponding author address: Dr. A. J. G. Nurser, Imperial College of Science and Technology, The Blackett Laboratory, Prince Consort Road, London SW7 2BZ, United Kingdom.

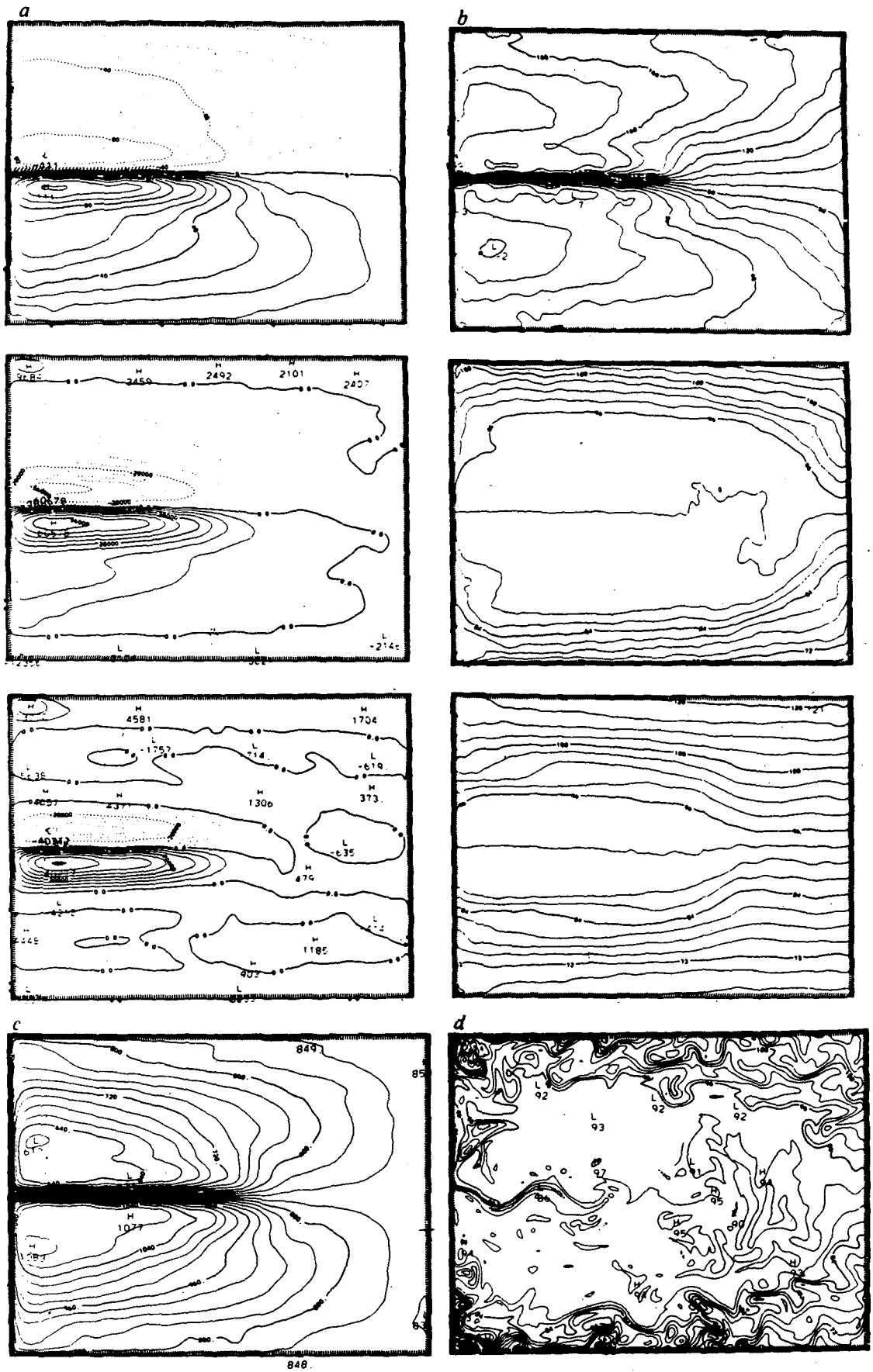
a
b
c
d
2492
2101
2407
4581
1704
1757
1306
373
635
1185
1077
849
848

In section 2 we investigate, without assuming quasi-geostrophy, the vertical structure of the circulation associated with a purely inertial Fofonoff gyre, where a homogeneous layer lies above a continuously stratified fluid. In section 3 we consider the modifications to the broad westward flow resulting from wind forcing.

2. The Fofonoff Gyre in a continuously stratified, non-quasi-geostrophic ocean

The presence of Fofonoff gyre-like flow in the upper layer of a quasi-geostrophic (Q-G) ocean has been shown (MN) to give rise to closed contours of Q-G potential vorticity q in the layer below. Inside these contours, homogenization of q is imagined to take place in the manner described by Rhines and Young (1982); henceforth RY. The resulting flow field is a system of "stacked" Fofonoff gyres; the "bowl" within which motion develops, and q is uniform, deepens northward toward the Gulf Stream (see Fig. 3). Outside the bowl, there is no flow.

These solutions are of most relevance to the recirculation of the subtropical gyre as seen in models and, for example, in the North West Atlantic between 15° and 40°N, 80° and 50°W. The inertial "eastern boundary current" of these Fofonoff-like circulation schemes should be regarded merely as a device to ensure mass balance and allow meridional flow to break the Sverdrup constraint. It represents the complex time dependent processes which in reality allow the circulation to be completed. It is the westward return flow and the western and northern inertial jets which are represented most realistically in these solutions.

Here we investigate the structure of such gyres where a continuously stratified fluid lies below the surface homogeneous layer. We do not assume quasi-geostrophy, and so order-one variations in layer depth are allowed. The vertical structure is determined following the development of the approach of RY by Pedlosky and Young (1983; henceforth PY). The position of the topmost isopycnal of the stratified fluid is assumed to be known. Given knowledge of the thicknesses of the moving stratified layers below (which, in the interior, trivially follows from an assumed potential vorticity distribution), one can calculate the depth of the bowl of moving fluid which is necessary to ensure that the isopycnals underneath lie flat. The entire density and velocity fields then follow.

The approach of RY and PY actually assumed knowledge of the depth-integrated transport rather than the position of the uppermost isopycnal; this yields a first-order differential equation for the position of the topmost isopycnal and/or the depth of the bowl. This approach is made use of in section 3 in considering the wind-induced perturbation of the bowl.

a. The model

Continuously stratified fluid is supposed to underlie an upper homogeneous layer in which there is a Fofonoff-like subtropical gyre: a broad westward return flow on the southern flank, together with inertial boundary currents to the west, north and east. It is assumed that such a solution is possible. Analytical study of the structure of the inertial jets becomes difficult, and so here we restrict detailed discussion to the interior. The inertial jets are only considered insofar as they affect the potential vorticity field through completing the circulation.

The subtropical gyres cover large areas over which the static stability shows very substantial horizontal variation. It is, therefore, inappropriate to assume quasi-geostrophy. Forcing and dissipation are considered only insofar as they yield

1) an Ekman pumping condition

$$w = w_0 \quad \text{at} \quad z = 0 \tag{2.1}$$

at the base of the mixed layer and

2) through integral balances over closed streamlines, a potential vorticity distribution in the stratified fluid. The three components of the momentum equation for steady flow are then, adopting local Cartesian coordinates x, y, z, with x eastwards, y northwards, z upwards, and corresponding velocity components u, v and w:

$$(\mathbf{u}\cdot\nabla)u - fv = -p_x/\rho_0 \tag{2.2a}$$

$$(\mathbf{u}\cdot\nabla)v + fu = -p_y/\rho_0 \tag{2.2b}$$

$$0 = -p_z - \rho_0(1 - g^{-1}B)g \tag{2.2c}$$

where p is the pressure, ρ_0 the mean density, B the (kinematic) buoyancy and g the gravitational acceleration. The velocity field is solenoidal

$$\nabla\cdot\mathbf{u} = 0 \tag{2.3}$$

and mass is conserved, so

$$(\mathbf{u}\cdot\nabla)B = 0. \tag{2.4}$$

It is assumed that outside the gyre the fluid is stratified according to a "reference stratification," and further, that this reference stratification is consistent with there being no motion and so is independent of the horizontal coordinates. The reference buoyancy profile is taken to be

$$B(z) = B_*, \quad -H < z < 0 \tag{2.5a}$$

FIG. 1. (a) Five-year mean streamfunctions in the top, third and fifth layers, respectively, of the 8-level eddy-resolving model of Holland. Reproduced from Holland et al., 1984. The gyres shrink and recede towards the line of symmetry with depth. (b) The mean Q-G potential vorticity on the three levels. On the deeper layers homogenization extends across both gyres. (c) The mean depth in meters of the third layer. (d) The instantaneous potential vorticity of the third layer.

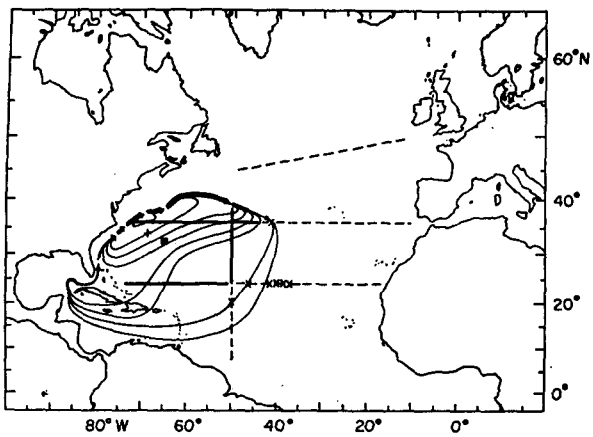

FIG. 2. Warm water (>17°C) circulation diagram of Worthington (1976, Fig. 42).

over the homogeneous upper layer of reference thickness H, and

$$B(z) = B_0(z), \quad z < -H \tag{2.5b}$$

in the underlying stratified fluid.

In order to ease comparison with the Q-G theory, and separate out the effects of stratification, (consideration of which is deferred to section 2b), we introduce the quasi-vertical coordinate z_0, defined by

$$B_0(z_0(B)) = B. \tag{2.6}$$

This z_0 "tags" an isopycnal by the position it held in the reference profile. The depth of the isopycnal $z = z(z_0, x, y)$ is now a dependent variable. In particular, the base of the mixed layer lies at $z = -h(x, y) = z(-H, x, y)$. (See Fig. 4.) Because z_0 "tags" the isopycnal, it, like density, is conserved.

Another conserved quantity (ζ is the relative vorticity $\mathbf{k} \cdot \nabla \times \mathbf{u}$) is

$$Q = (\zeta + f)\frac{dz_0}{dz} = (\zeta + f) \Big/ \left(\frac{dz}{dz_0}\right) \tag{2.7}$$

which is asymptotic to the Q-G potential vorticity q in the Q-G limit. We shall henceforth describe Q as "potential vorticity." Except in the boundary currents and, possibly, the tight recirculation immediately south of the Gulf Stream, the contribution of relative vorticity is insignificant, and Q is well approximated by $f dz_0/dz$.

The key assumptions which allow the determination of the vertical structure within the stratified fluid are (RY, MN, PY) that

1) the flow is quasi-free: sources and sinks of Q are, formally, vanishingly weak but

2) the balance between these sources and sinks constrains the potential vorticity distribution.

In particular, eddies are assumed to transfer Q laterally downgradient (RY, MN). This may be interpreted as resulting from eddy form drag, with the collusion of lateral Reynolds stresses where relative vor-

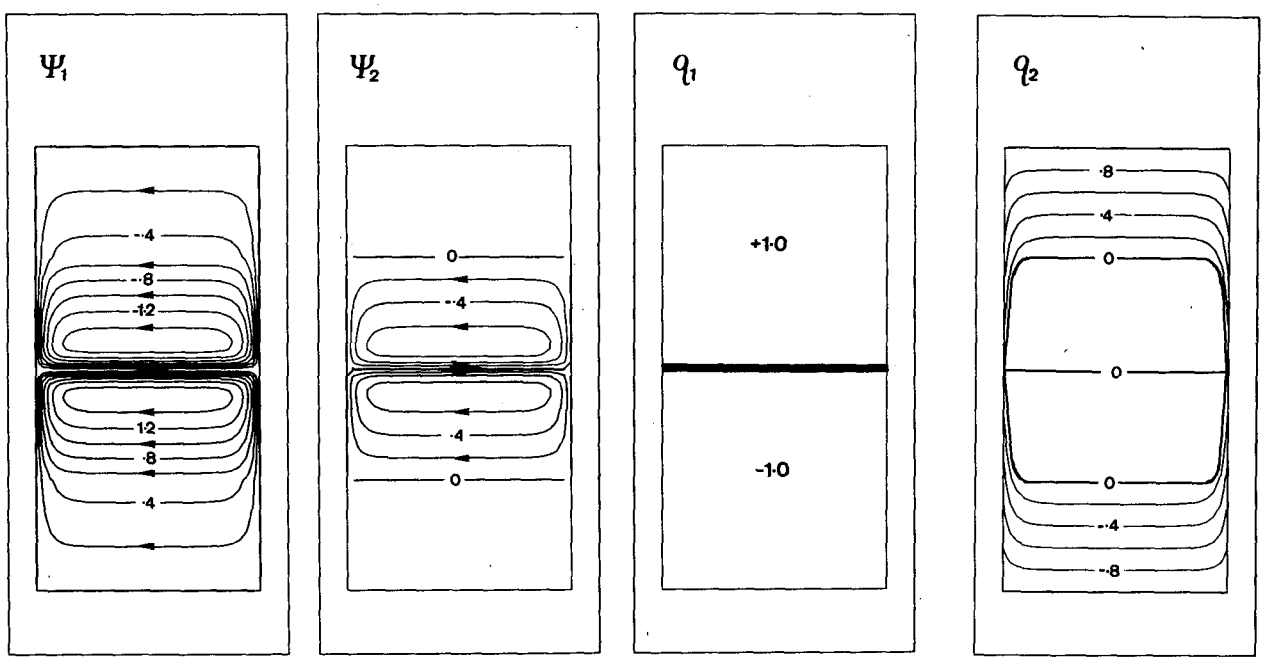

FIG. 3. A plan view of the 2½ layer, double baroclinic Fofonoff gyres of MN (Fig. 7). The meridional extent of the double gyre is $2L$, and the internal Rossby radius L_e. The Q-G streamfunction is plotted in units of $\beta L_e^2 L$ (a) ψ_1 in the upper layer and (b) ψ_2 in the lower moving layer (ψ_2), and the Q-G potential vorticity in units of βL; (c) q_1 in the upper layer and (d) q_2 in the lower moving layer.

ticity is important. Closed contours of quasi-free flow set a boundary condition Q = constant which allows geostrophic eddies to homogenize Q everywhere inside the outermost closed contour of such flow on a given isopycnal surface. Hence, it is assumed that Q is uniform on an isopycnal surface wherever that surface is displaced from its reference position.

The determination of the value to which Q is homogenized is less clear. The argument in the original paper of RY assumes that relative vorticity is unimportant. It is clearest in a layered model. Assume initially that all the barotropic transport is carried in the surface layer. Contours of f/h_2, where h_2 is the thickness of the layer immediately below, are distorted by the variation of upper layer thickness h_1 associated with the flow there. Some of these contours close and act as "rails" along which eddy form drag accelerates flow. This eventually has the effect of homogenizing Q inside these contours, but it cannot change the value of Q on the outermost initially closed contour, along which h_2 is fixed by h_1. This h_1 can be calculated from the barotropic streamfunction (RY) or from the potential vorticity distribution in the surface layer (MN). The same argument holds as we proceed to greater depths and consider the closure of Q contours in the layer below each newly homogenized layer. So the value to which Q is homogenized in each layer is unambiguously calculable.

But this is no longer necessarily the case if relative vorticity can contribute to Q as in the baroclinic Fofonoff gyres of MN. For instance, suppose relative vorticity becomes significant under the northern boundary current of a Fofonoff-like subtropical gyre. Then the value of relative vorticity on the northern "leg" of the outermost closed contour of Q determines the position of the southern leg (where relative vorticity is insignificant). The outermost closed contour of Q may now no longer coincide with the outermost *initially* closed contour, and so the value of Q along it and hence inside it may change also.

In the Q-G model of MN, in which equal sized subtropical and subpolar gyres were supposed to lie "back to back," it was possible to argue that eddy transfer across the separated Gulf Stream would ensure that the value of q to which homogenization took place would be the same in both gyres. By symmetry this value of $q = f_0$, the planetary vorticity characteristic of the inertial jet. Moreover, this value is the same on all isopycnals. Certainly this is spectacularly evident in the double-gyre Q-G eddy-resolving models (see Fig. 1).

But this symmetry develops only in a Q-G model with a double gyre. Thus $q = f_0$ may not be appropriate to the real ocean. Although there is evidence (Bower et al., 1985; Hogg et al., 1986) to suggest a tendency for potential vorticity to homogenize across the Gulf Stream at lower levels, the real ocean is far from symmetric. Subpolar gyres are far weaker than the subtropical gyres. Isopycnals surface; there is topography, and a thermohaline source-sink circulation, particularly strong in the Atlantic, which threads through the separated jet.

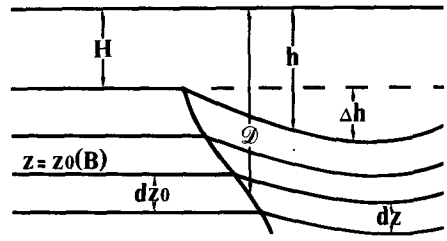

FIG. 4. To the left of the figure the fluid is motionless and the reference stratification $B = B_0(z)$ is expressed, with isopycnals lying at their reference depths $z = z_0(B)$, and the base of the surface layer at $z = -H$. The depression Δh of the base of the surface layer to the new position $z = -h$ pushes down the isopycnals. However, the potential vorticity distribution is such that the infinitesimal thickness between the isopycnals in the moving fluid (dz) is generally less than in the reference stratification (dz_0), so allowing the reference stratification to be recovered along the surface $z = z_0 = -\mathcal{D}$ which defines the "bowl."

Despite these uncertainties, we investigate here the problem in which "Fofonovian" flow in the surface homogeneous layer overlies stratified fluid in which on every isopycnal $Q = f_0 = f_N$, the value of planetary vorticity under the northern edge of the eastward-flowing jet. The effects of deviations from this Q distribution are discussed later.

b. *The baroclinic Fofonoff gyre*

The upper homogeneous layer of the model ocean, bulging down in response to Ekman pumping, is imagined to be in Fofonovian anticyclonic motion; thus the interface between it and the stratified fluid below is depressed by $\Delta h = h - H$ below its reference height $z = -H$ (see Fig. 4).

We assume for the present that Δh is known. The base of the bowl $z = -\mathcal{D} = z_0$ marks the boundary between the undisturbed fluid below, in which $Q = f$, and the fluid in motion, which has had its potential vorticity homogenized to $f_0 = f_N$ (the value of f under the Gulf Stream). Note $f_N > f$; hence inside the bowl, from (2.7), neglecting relative vorticity

$$\frac{dz_0}{dz} \approx \frac{f}{Q} = \frac{f}{f_0} < 1. \tag{2.8}$$

The stratified layers beneath are compressed. The bowl $z = z_0 = -\mathcal{D}$ marks the depth at which the accumulated squashing of these layers cancels out the depression of the top interface, and allows the stratification to return to its reference value.

Inside the region of homogenized Q we can integrate (2.8) downwards from the base of the surface layer, to

give the position of the isopycnal whose reference depth was z_0 as

$$z = -h + \frac{f}{f_0}(H + z_0) \tag{2.9}$$

and the displacement as

$$\Delta z = z - z_0 = -\Delta h - (1 - f/f_0)(H + z_0). \tag{2.10}$$

The displacement (downward and therefore negative) of the isopycnal is given by the surface layer base displacement, less the relative loss of thickness $(1 - f/f_0) \times$ the reference thickness of the squashed layers in between. The bowl is defined by the surface along which $z = z_0 = -\mathcal{D}$; hence from (2.10)

$$\mathcal{D} - H = \Delta h/(1 - f/f_0). \tag{2.11}$$

The independence of $\mathcal{D}$ from the stratification is worthy of note and holds *only if* the h field is unaffected by the flow in the stratified fluid beneath the mixed layer. Where, as in the theory of RY, the total depth integrated circulation is constrained by Sverdrup balance, the h field does depend on this flow, but of course (2.11) still holds. The "free" nature of the Fofonoff-like circulations considered here, in which inertial boundary currents handle whatever meridional transport is implied by the stratification, make it possible for the surface thickness field to be set by a constraint such as uniform potential vorticity. Of course, where the potential vorticity (and hence thickness distribution) in the upper layer is dependent on the streamfunction there, then the h field and hence the shape of the bowl beneath again depend on the stratification.

Let us consider such a Fofonovian circulation in the upper layer in which the potential vorticity is everywhere constant and equal to the value f_S/H appropriate to the layer taking up its reference thickness H at the southern edge of the gyre where $f = f_S$ and relative vorticity is unimportant. This negative perturbation to the potential vorticity in the surface layer reflects the effect of the Ekman pumping over the subtropical gyre. The slightly unrealistic assumption that f/h is uniform is made here for the sake of simplicity. The perhaps more realistic case in which potential vorticity in the upper layer is supposed to decrease towards the center of the gyre is considered later.

Thus, where ζ may be neglected

$$f/h = f_S/H$$

$$\Delta h = H(f - f_S)/f_S. \tag{2.12a}$$

Therefore

$$\mathcal{D} = H\frac{f}{f_0}\left(\frac{f_0}{f_S} - 1\right)\left(1 - \frac{f}{f_0}\right). \tag{2.12b}$$

The resultant isopycnal field and "bowl" are shown in Fig. 5 for a subtropical gyre extending from 15° to 40°N with an upper layer of reference thickness H = 150 m. From the form of (2.11), it is clear that, south of the eastward-flowing Gulf Stream analogue in which the contribution made by relative vorticity towards potential vorticity allows relaxation of the depression of the base of the upper layer, (and indeed modifies the required stretching in the stratified fluid itself), $\mathcal{D}$ is bound to increase in a roughly hyperbolic manner as f approaches f_0, the "stem" of the champagne glass seen in the vertical sections across the multilayer Q-G numerical models. The obvious question is: does the bowl strike the ocean floor? The answer depends on 1) how large is the Δh calculated by excluding relative vorticity close to the jet, where $f \approx f_0$ leads to a deep bowl being necessary to nullify the imposed squashing [see (2.11)] and 2) the meridional extent of the eastward jet, which determines how far south of the axis of the jet this Δh is expressed.

For a subtropical gyre 15°–40°N, H = 150 m, (2.12a) gives a maximum Δh = 220 m. Then the bowl strikes the ocean floor (assumed to lie at a depth of 4500 m) where

$$\frac{f_0 - f}{f_0} = \frac{\Delta h}{\mathcal{D} - H} = \frac{220}{4350}. \tag{2.13}$$

This gives a latitude about 37.5°, which is 2.5° or 270 km south of the northward rim of the inertial jet. So if the eastward jet is less than 200 km thick, the bowl will strike the bottom.

The precise width of the jet can only be determined numerically; however, we would expect it to be of the same order as in a layered model. In the Q-G layered model of MN, the width of the upper layer jet was found to be $(U/\beta)^{1/2}$, U being an estimate of the maximum westward velocity in the interior westward flow. For U = 20 cm s^{-1} (a comfortable overestimate of the velocities in the interior) and $\beta \sim 10^{-11}$ m^{-1} s^{-1} this would give a width of ~140 km.

So the theory predicts that the bowl does strike the ocean floor, a couple of hundred kilometers south of the inertial jet—if it is assumed that potential vorticity is constant in the upper layer and that the deep Q is homogenized to the value of the planetary vorticity under the inertial jet.

However, there is evidence that f/h decreases towards the center of the gyre as is seen, e.g., in the map of potential vorticity calculated between σ_t = 26.3 and 26.5 by McDowell et al. (1982), or results from Q-G eddy resolving models as in Fig. 1. With such an upper layer potential vorticity distribution the bowl may strike further south. For example, taking a maximum h of 500 m and a Δh of 350 m, as might be suggested by the *Atlantis* section across the Gulf Stream at 50°W, reproduced as Fig. 3 of McCartney (1982), implies that the bowl strikes the floor ~420 km south of the jet. A barotropic circulation is excited over the region north of where the bowl strikes the floor: this is discussed in Marshall and Nurser (1988); henceforth MNII.

Linkage of the analytical models to the behavior of Q-G models is relatively straightforward. It is evi-

dent—see Fig. 1—that here, in the lower layers where they are in motion, *q does* become homogenized to the value appropriate to undisturbed fluid under the axis of the separated jet.

The observations in the northwest Atlantic seem to imply that there is a barotropic recirculation with a meridional extent of a few degrees (Schmitz 1980, Hogg 1983, Richardson 1985). This is consistent with the bowl hitting the floor according to the preceding calculation. The barotropic circulation carries a large fraction of the "overspun" transport and has a meridional scale small enough that relative vorticity probably plays a role in its dynamics. It is, however, far less clear that the wind-driven circulation penetrates to the floor of the Pacific Ocean (Niiler et al., 1985). This is consistent with the much less marked downward depression of the isotherms seen, for instance, in the section across the Kuroshio at 155°E, which appears as Fig. 1 of Masuzawa (1969).

Our estimate of the depth of penetration of the gyre is surprisingly good, given the dubious validity in the real oceans of the assumptions behind the preceding calculation. It is not clear that in fact potential vorticity is necessarily uniform on the deeper surfaces where they are in motion—see again the Atlantis 50°W section. Even where Q is homogenized, there is no reason in an asymmetrical ocean for it to take the value of f under the Gulf Stream, and the extreme sensitivity of the depth of the bowl to the value of Q is apparent from (2.13).

c. *The velocity fields*

Away from the inertial jets the velocity fields can be calculated straightforwardly; our treatment follows that of PY. The thermal wind equations may be written

$$fv_z = B_x = \frac{dB_0}{dz_0} z_{0x}$$

$$fu_z = -B_y = -\frac{dB_0}{dz_0} z_{0y}$$

in terms of z_0. It should be noted that only the zonal velocities are nonzero in the interior of the "free" Fofonoff gyre of Fig. 5, but we also derive expressions for the meridional velocities as these are nonzero when the gyre is forced. Making use of the partial differential relation

$$\left(\frac{\partial z_0}{\partial y}\right)_{z,x} = -\left(\frac{\partial z}{\partial y}\right)_{z_0,x} \Big/ \left(\frac{\partial z}{\partial z_0}\right)_{x,y}$$

and the similar reexpression of $\partial z_0/\partial x$ yields

$$fv_{z_0} = -\frac{dB_0}{dz_0} z_x \tag{2.14a}$$

$$fu_{z_0} = \frac{dB_0}{dz_0} z_y. \tag{2.14b}$$

Here z_x, z_y are the slopes of the isopycnals with "reference depth" z_0. We then substitute (2.11) into (2.9) to express z in terms of z_0 and $\mathcal{D}$, the depth of the bowl; (2.14) then becomes

$$fv_{z_0} = \frac{dB_0}{dz_0}\frac{\partial}{\partial x}(z_0 - z) = \frac{dB_0}{dz_0}\frac{\partial}{\partial x}[(1 - f/f_0)(\mathcal{D} + z_0)] \tag{2.15a}$$

$$fu_{z_0} = -\frac{dB_0}{dz_0}\frac{\partial}{\partial y}(z_0 - z)$$

$$= -\frac{dB_0}{dz_0}\frac{\partial}{\partial y}[(1 - f/f_0)(\mathcal{D} + z_0)]. \tag{2.15b}$$

Integrating up from $z_0 = -\mathcal{D}$, where $u = v = 0$, and taking the $\partial/\partial x$ and $\partial/\partial y$ outside the integral furnishes

$$fv = M_x|_{z_0}, \quad fu = -M_y|_{z_0} \tag{2.16}$$

where the Montgomery potential M is given by

$$M = \int_{-\mathcal{D}}^{z_0} (1 - f/f_0)(\mathcal{D} + z_0)\frac{dB_0}{dz_0}\, dz_0. \tag{2.17}$$

If $\mathcal{D}$ is varying on the same scale as f, then

$$u \sim \beta_* N_*^2 H_*^2 / f_*^2.$$

Choosing plausible values $N_* = 2 \times 10^{-3}$ s^{-1} (equivalent to a density gradient of 0.4 kg m^{-3}/km), $H_* = 1$ km and values of β_* and f_* appropriate to 27.5°N gives a velocity scale $U_I = 1.79$ cm s^{-1}.

In Fig. 5, the velocity field associated with the Fofonoff gyre has been plotted in units of this U_I. It is everywhere westward and ranges up to a few cm s^{-1}, strengthening towards the surface and the north as additional shear contributes towards it. Note that this is the baroclinic (i.e., that associated with the buoyancy gradients) velocity field.

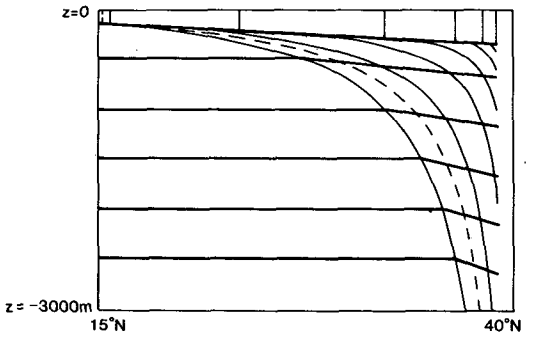

FIG. 5. A north–south cross section across the Fofonoff gyre. The hyperbolic stratification (2.18) is supposed, with a scaled buoyancy jump $\Delta B' = 2$ (for details, see text), equivalent to a density jump of 0.8 kg m^{-3}, between the stratified fluid and the upper homogeneous layer. Isopycnals are denoted by thick lines and contours of (westward velocity) by thin lines. The contour interval is in units of the "inertial" velocity scale U_I (1.79 cm s^{-1}); the dashed line indicates the $0.5U_I$ contour. The zero contour of velocity marks the edge of the "bowl."

The depth integrated transport, south of where the bowl is predicted to attain a depth of 4500 m and hence strike the bottom, is about 44 Sv in this case in which potential vorticity is supposed constant in the upper layer. North of this, the barotropic circulation which is excited (MNII) modifies the present theory, and is associated with a large transport which probably makes up the bulk of the recirculation.

Where the thickening of the mode waters is marked enough that potential vorticity in the upper layer actually decreases northwards, the implied transport increases: choosing a reasonably realistic maximum depression (see again the Atlantis section) $\Delta h = 350$ m yields a transport 80–85 Sv.

The reference stratification adopted in the computation of Fig. 5 and the above transports is a modification of the "hyperbolic" stratification introduced by Gill (1984) viz.

$$B_0(z) = \begin{cases} B_{\text{ref}} + \Delta B, & z > -H \\ B_{\text{ref}} + s^2[(H_s + H)^{-1} - (H_s - z)^{-1}], & z < -H. \end{cases} \tag{2.18a}$$

Here H is the thickness of the homogeneous surface layer, and s and H_S are empirically derived quantities chosen to give a good match to the observed stratification. Throughout we follow Gill in choosing $s = 2.81$ m s^{-1}, but choose $H_S = 150$ m rather than his value of 140 m. The implied total buoyancy difference between 5000 and 150 m is 27×10^{-3} m s^{-2}—a density difference of 2.7 kg m^{-3}. This stratification may be alternatively written in scaled form

$$B'_0(z') = \begin{cases} B'_{\text{ref}} + \Delta B', & z' > -H' \\ B'_{\text{ref}} + \alpha[(H'_s + H')^{-1} - (H'_s - z')^{-1}], & z' < -H' \end{cases} \tag{2.18b}$$

where H'_S, H' and z' have been scaled by H; B'_{ref} and $\Delta B'$ by $H_* N_*^2$ and $\alpha = s^2/(H_* N_*)^2$. In our calculations the value of the buoyancy jump underneath the surface layer will be varied: in Fig. 5 a value $\Delta B = 8 \times 10^{-3}$ m s^{-2} (a scaled value of $\Delta B' = 2$), corresponding to a density jump of 0.8 kg m^{-3}, has been chosen.

It is interesting to compare the corresponding results for uniformly stratified fluid. Consider an alternative expression for u, derived by direct integration of (2.14a) using the expression (2.9) for the isopycnal height z

$$u = -\frac{f_*}{f} U_I \frac{f_*}{\beta_*} \int_{-\mathcal{D}'}^{z'_0} \frac{\partial z'}{\partial y} \frac{dB'_0}{d\tilde{z}'_0} d\tilde{z}'_0$$

$$= -\frac{f_*}{f} u_I \frac{f_*}{\beta_*} \int_{-\mathcal{D}'}^{z'_0} \frac{\partial}{\partial y}[h' - (\tilde{z}_0 + H')f/f_0] \frac{dB'_0}{d\tilde{z}_0} d\tilde{z}_0.$$

This illustrates how the velocity is built up from integration of the shear: the product of the isopycnal slope and the buoyancy gradient. With a realistic stratification, the strong stratification near the surface acts on less marked isopycnal slopes. If a uniformly stratified model is to give realistic velocities where the bowl attains reasonable depth, it must underestimate the stratification. Results are plotted in Fig. 6 (again in units of U_I) for a buoyancy gradient 2×10^{-6} s^{-2} (0.2 kg m^{-3}/km). Velocities in the recirculation are seen to be of similar order to those in Fig. 5; of course, they are grossly underestimated where the bowl is shallow. Since the velocities are proportional to the stratification, the results in Fig. 6 can be reinterpreted as deriving from a gradient of say, 0.8 kg m^{-3} km, more appropriate to the upper ocean, if we suppose a value of $U_I = 7.2$ cm s^{-1}. In this case the recirculation velocities are grossly overestimated close to the stream.

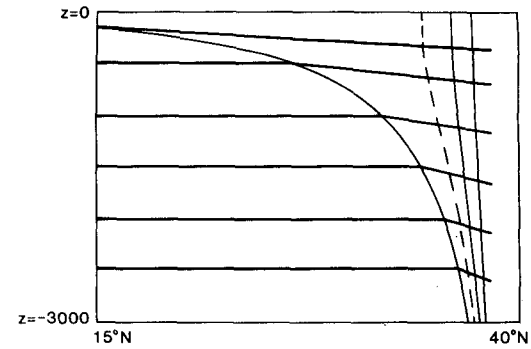

FIG. 6. As in Fig. 5 except that a uniform stratification with density gradient 0.2 kg m^{-3} km^{-1} is supposed without a buoyancy jump. Scaling as in Fig. 5.

3. The modification of the free circulation by wind

The thickness of the surface layer is (in the interior) solely a function of latitude in the free Fofonoff gyre considered in the preceding section. This implies circulation which is purely zonal except in the assumed eastern and western boundary currents, and therefore that potential vorticity is conserved everywhere in the surface layer.

We now suppose that a wind stress τ acts upon the surface layer. This drives an Ekman flux whose divergence must be balanced by the divergence of a geostrophic flow. We consider only the geostrophic component, so, if the effect of the wind stress is restricted to the mixed layer, we can adopt a formalism in which the wind stress acts solely through the Ekman suction

$$w_0 = w|_{z=0} = \mathbf{k} \cdot \text{curl}[\tau/(\rho_0 f)] \tag{3.1}$$

at the top of the surface layer.

In the subtropical gyre, the convergent Ekman flux drives Ekman pumping which pushes down the interface between the surface layer and the water below in the classic manner. Potential vorticity is no longer conserved along streamlines in the surface layer, but

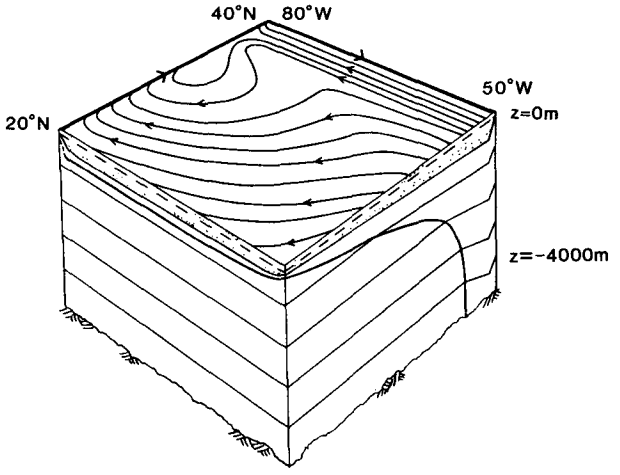

FIG. 7. A block diagram of the flow associated with a distorted Fofonoff gyre, looking from the southeastern corner. The flow is supposed to enter along the eastern flank as if from a "free" Fofonoff gyre; hence the hyperbolic shape of the bowl. The flow is driven south by the wind stress curl; hence the bowl deepens westwards. The circulation is completed by an inertial WBC and separated jet.

the fluid remains shielded from forcing in the layer below. It is thus possible to argue that potential vorticity is again homogenized and so (2.11) still gives the depth of the bowl, which is now a function of x and y.

The wind stress acts on the westward flowing water in the interior. As in the previous section, the water which appears at the eastern boundary of the region under consideration—an analogue of, say, the northwest corner of the Atlantic—is supposed to enter from the east as if from an inertial eastern boundary current, an idealization of the complex processes which serve to return the recirculating waters.

The flow then, is purely zonal at the eastern boundary. As in section 2 the surface layer thickness is specified as a function of latitude—in the simplest case potential vorticity is constant, with a value equal to that found at the southern edge of the gyre where the surface layer thickness is equal to its reference thickness. The depth of penetration of the bowl and the displacement of the isopycnals along this line then follow. The flow and density fields are pictured schematically in Fig. 7.

From the Ekman pumping velocity in the wind-influenced region we may calculate the vertically integrated meridional transport. But the slopes of all the isopycnals in the stratified fluid, and hence also this meridional transport are determined by the position and slope of the interface between the surface layer and the fluid below (or indeed by the position and slope of the bowl). A differential equation may thus be constructed (PY) that links some function of h and h_x, or $\mathcal{D}$ and $\mathcal{D}_x$ to the Ekman suction w_0. This may then be integrated from the eastern boundary to give fields of h (or $\mathcal{D}$) and therefore the complete flow. Rather than imposing an eastern boundary condition of no flow as in PY, we "inject" fluid from the east as if from the baroclinic Fofonoff gyre of section 2. Here we work with $\mathcal{D}$ rather than h in agreement with PY. Once we have found the $\mathcal{D}$ field, the density and velocity fields are, of course, calculable everywhere.

Integration of the Sverdrup relation $f\partial w/\partial z = \beta v$ gives

$$\int_{z=-\mathcal{D}}^{0} v(z)dz = \int_{z_0=-\mathcal{D}}^{z_0=-H} v(z_0)ff_0^{-1}dz_0 + h\tilde{v} = fw_0/\beta$$

where $\tilde{v}$ is the velocity in the surface layer and use has been made of the postulate that Q is constant in the stratified fluid, which requires that $dz/f = dz_0/f_0$. But by (2.16) and (2.17)

$$v(z_0) = \frac{\partial}{\partial x}\left\{\frac{1}{f}\int_{-\mathcal{D}}^{z_0}(1 - f/f_0)(\mathcal{D} + z_0)\frac{dB_0}{dz_0}\,dz_0\right\}$$

and from an integration of (2.14a) over the (possible) buoyancy jump at the base of the surface layer

$$\tilde{v} - \lim_{z_0 \uparrow -H} v(z_0) = \frac{1}{f}\Delta B \cdot h_x.$$

After some manipulation, we find

$$(1 - f/f_0)\frac{\partial}{\partial x}\left[\int_{-\mathcal{D}}^{-H}\left\{\int_{-\mathcal{D}}^{z_0}(\mathcal{D} + \tilde{z}_0)\frac{dB_0}{d\tilde{z}_0}\,d\tilde{z}_0 + \frac{1}{2}(1 - f/f_0)(\mathcal{D} + z_0)^2\frac{dB_0}{dz_0} + H(\mathcal{D} + z_0)\frac{dB_0}{dz_0}\right\}dz_0\right.$$
$$\left. + \frac{1}{2}\Delta B.(1 - f/f_0)(\mathcal{D} - H)^2 + \Delta B.H(\mathcal{D} - H)\right] = f^2 w_0/\beta. \quad (3.2)$$

For uniform stratification, where $dB_0/dz_0 = N^2$ this reduces to Eq. (2.30) of PY.

The quantity inside the square brackets can be determined by integration of (3.2) from the eastern boundary. In the numerical calculations presented here, values of $\mathcal{D}$ were then recovered by a Newton–Raphson scheme from an analytic expression for the quantity inside the brackets.

It is advantageous to rewrite (3.2) in terms of the scaling introduced in section 2. We further introduce W_0 as an Ekman pumping scale, and hence $U_S = f_* W_0/(\beta_* H_*)$ the Sverdrup velocity scale. For an Ekman pumping $W_0 \sim 1.5 \times 10^{-4}$ cm s^{-1} (12 cm day^{-1}), a length scale $L_* = f_*/\beta_* \approx 3300$ km and a depth scale $H_* = 1000$ m, this gives $U_S \sim 0.5$ cm s^{-1}: the Sverdrup velocity if all the flow were concentrated in the upper 1000 m.

Then (3.1) becomes, writing $w_0' = w_0/W$, $\mathcal{D}' = \mathcal{D}/H_*$, $H' = H/H_*$

$$L_* \frac{\partial}{\partial x}\left[\int_{-\mathcal{D}'}^{-H'}\left\{\int_{-\mathcal{D}'}^{z_0'}(\mathcal{D}'+\tilde{z}_0)\frac{dB_0'}{d\tilde{z}_0}\,d\tilde{z}_0 + \tfrac{1}{2}(1-f/f_0)(\mathcal{D}'+z_0')^2\frac{dB_0'}{dz_0'} + H'(\mathcal{D}'+z_0')\frac{dB_0'}{dz_0'}\right\}dz_0' + \tfrac{1}{2}\Delta B'\cdot(1-f/f_0)(\mathcal{D}'-H')^2 + H'\cdot\Delta B'\right] = \frac{U_S}{U_I}\frac{\beta_*}{f_*^2}\frac{f^2}{\beta}\frac{w_0'}{(1-f/f_0)}.$$

The spatial scales are large enough that, strictly, it is necessary to plot in terms of latitude θ and longitude λ, in which case $\mathcal{D}'$ may be determined by integration of

$$\frac{\partial}{\partial\lambda}\left[\int_{-\mathcal{D}'}^{-H'}\left\{\int_{-\mathcal{D}'}^{z_0'}(\mathcal{D}'+\tilde{z}_0)\frac{dB_0'}{d\tilde{z}_0}\,d\tilde{z}_0 + \tfrac{1}{2}(1-f/f_0)(\mathcal{D}'+z_0')\frac{dB_0'}{dz_0'} + H'(\mathcal{D}'+z_0')\frac{dB_0'}{dz_0'}\right\}dz_0' + \tfrac{1}{2}\Delta B(1-f/f_0)(\mathcal{D}'-H')^2 + H'\cdot\Delta B'\right] = \frac{U_S}{U_I}\frac{\beta_*}{f_*^2}\frac{f^2}{\beta}\frac{w_0'}{(1-f/f_0)}. \quad (3.3)$$

a. Results

We present numerically evaluated density and velocity fields inside a domain of latitudinal extent 15°–40°N, and 30° in longitudinal extent. This corresponds to the region "fed" by the eastern boundary current and identified with, say, in the North Atlantic, the region between 80° and 50°W. A classical sinusoidally varying Ekman pumping field is chosen over this subtropical gyre in which the Sverdrup velocity is everywhere southward. Thus

$$w_0' = -\sin[\pi(\theta-\theta_S)/(\theta_N-\theta_S)] \quad (3.4)$$

where $\theta_N = 40°$, $\theta_S = 15°$ and the maximum pumping occurs at 27.5°N. In the following calculations we have set $U_S/U_I = 1$, which is probably an overestimate. With stratification of the strength adopted here, $U_S \sim 1.8$ cm s^{-1}, so $W_0 \sim 5\times10^{-4}$ cm s^{-1} $\sim$ 45 cm day^{-1}. This is rather larger than the maximum of 12 cm day^{-1} of Leetmaa and Bunker (1978). However, this implied overestimated w_0 (and/or underestimated stratification) emphasizes the effects of Ekman pumping, and since it is zonally independent, simply serves to shorten the distance from the eastern boundary at which a given displacement of the isopycnals from their level at the eastern boundary occurs.

Initially we assume the "realistic" stratification (2.18) with no density jump at the interface with the surface layer: $\Delta B' = 0$.

Contours are plotted of $\mathcal{D}$, the depth of the bowl, in Fig. 8. The wind driving is seen to deepen the bowl towards the west. The mechanism behind this deepening, discussed here, is clarified by inspection of the zonal cross section Fig. 9a—at 20°N—and 9b—at

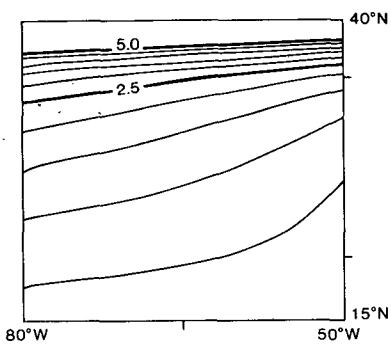

FIG. 8. Contours of the depth of the bowl measured in kilometers, C.I. = 0.5 km. The hyperbolic stratification (2.18) is supposed, without a buoyancy jump underneath the surface layer. The tick mark along the southern boundary lies at 65°W, and those along the eastern boundary at 20° and 35°N.

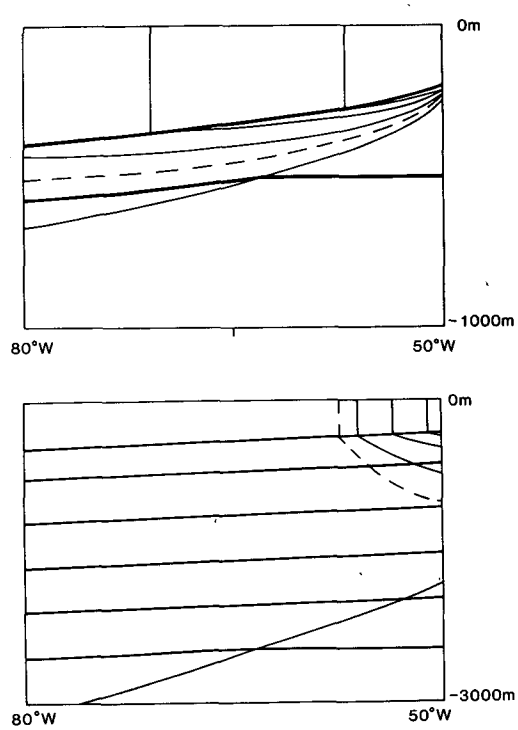

FIG. 9. Zonal sections across the bowl at (a) 20°N and (b) 35°N. Thick lines mark the isopycnals; thin lines contours of southward velocity. The contour interval in (a) is $0.2U_I$, with the dashed line at $0.1U_I$ and in (b) is $0.1U_I$ with the dashed line at $0.05U_I$. Stratification as in Fig. 8.

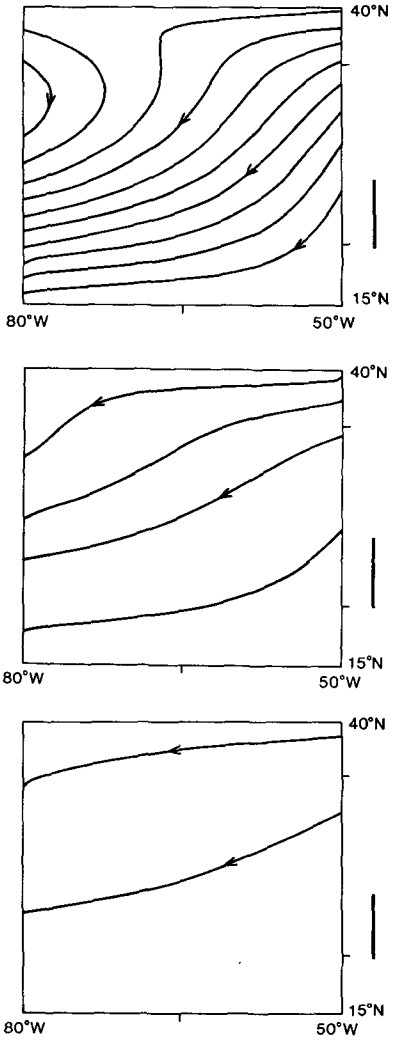

FIG. 10. Contours of $M/(f_* U_I L_*)$, where M is the Montgomery potential, f_* is the value of f at 27.5°N, $L_* = f_*/\beta_*$ with β_* the value of β at 27.5°N, and $U_I = 1.79$ cm s^{-1}. Contour interval is 0.2. The length of the line on the right of the figures then represents the distance between these contours (at 27.5°N) which implies a velocity U_I. (a) On the isopycnal surface $z_0 = -H = -150$ m just below the surface layer; this is equivalent to contours of (similarly scaled) pressure in the surface layer, since there is no buoyancy jump. (b) on the isopycnal surface $z_0 = -500$ m. Note the zero contour defines the edge of the bowl. (c) on the isopycnal surface $z_0 = -1000$ m. Tick marks are as in Fig. 8.

35°N. The uniformity of f/dz requires that the isopycnals lie parallel in the zonal sections, so the meridional shear must everywhere retain the same sense, that of the Sverdrup transport.

The isopycnals, including the interface with the surface layer, thus tilt downwards towards the west. Since $\mathcal{D} - H$ is proportional to the downward displacement of the interface, the bowl also must deepen westwards.

The barotropic meridional transport is zonally independent. The meridional velocities, which themselves decline westwards as the bowl deepens and the Sverdrup transport spreads vertically, are of order isopycnal tilt × depth of stratified fluid in motion (since $\Delta B = 0$). The isopycnals thus steepen where the bowl is shallow. Indeed if, as in PY, a condition of no motion is assumed along the eastern coast, so that $h = H = \mathcal{D}$ there everywhere, then a "tulip" shaped bowl appears, which descends vertically at the eastern coast.

The variation with depth of the flow fields is best seen in the plots of the Montgomery function on various isopycnal surfaces in Fig. 10. Note the clockwise rotation with increasing depth: the so-called "β-spiral" (Stommel and Schott, 1977) associated with the downward motion driven by the Ekman pumping.

The meridional variation, however, is the most interesting. Both in Fig. 10, and in the meridional cross-section Fig. 11, it is evident that the zonal flow has been much distorted from the pure Fofonoff flow (Fig. 6) present along the line of entry to the east. The sinusoidal wind stress curl field generates a classical Sverdrupian zonal flow, which is eastward north of the latitude of maximum Ekman pumping (more accurately the maximum of $-fw_0/\beta$) and westward to the south of it. Strengthening as we move westwards, it is responsible for the region of eastward flow close to the surface seen at 80°W (Fig. 11b). Note that in this unventilated model, whether or not the streamlines in the stratified fluid reach the eastern boundary, they are still

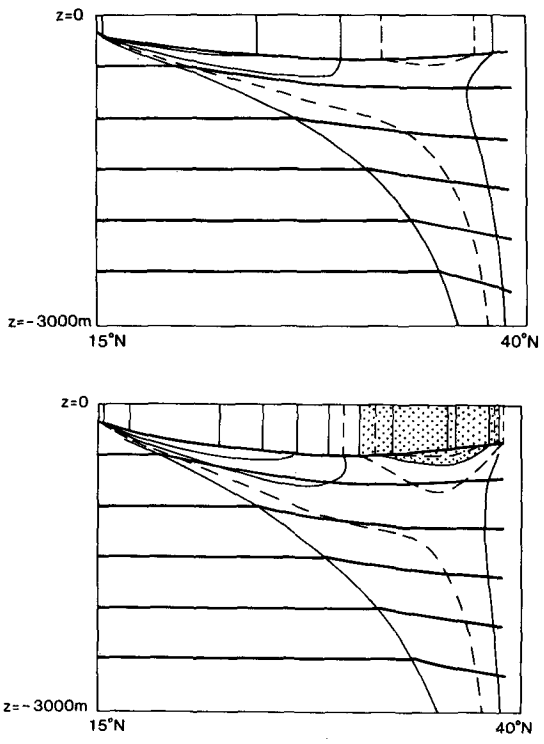

FIG. 11. Meridional cross sections across the gyre at (a) 65°W and (b) 80°W. Stratification as in Fig. 8. Westward velocity contoured in units of $U_I = 1.79$ cm s^{-1}; the dashed line indicates the $0.5U_I$ contour. Reversed (eastward) flow is stippled.

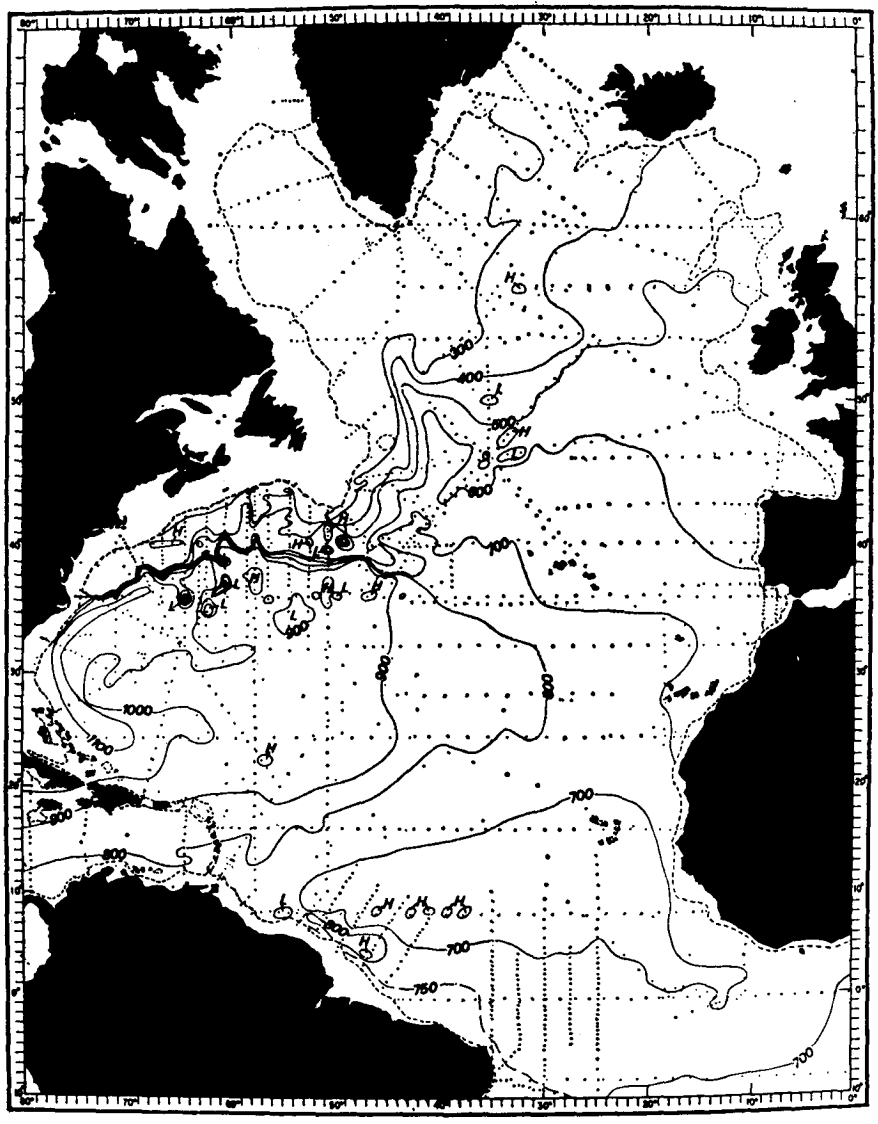

FIG. 12. Relative topography of 100 db relative to 700 db (dynamic millimeters). Reproduced from Fig. 2 of Stommel et al. (1978).

closed and eddy processes still homogenize Q inside them—there is thus no change in the flow regime depending on whether streamlines originate from the eastern or western coasts.

The striking feature about the density field is the downward bulge of the surface layer. This arises from the maximum of southward meridional flux at ~30°N, which yields a maximum in the rate of westward deepening of the bowl. This deepening is cumulative and hence much more marked at 80°W than 65°W.

It seems natural to identify this downward bulge of the near surface isopycnals, representing anticyclonic shear, with the southern lobe of the "C" elucidated by Reid (1981) in the dynamic topography of the subtropical gyres. See the lobe of 1000 and 1100 millimeter contours off Florida in the 100–700 db relative dynamic topography of Stommel et al. (1978) reproduced here as Fig. 12. This lobe does indeed seem to lie over the maximum of Ekman pumping (cf. Fig. 2 of Leetmaa and Bunker, 1978).

The mean velocity fields along 55°W synthesized by Richardson (1985) and presented in his Fig. 6b actually include a region of eastward velocities, at about 33°N. However, it is occurring at the eastern edge of the recirculation. The eastward velocities rather may be associated with the southernmost counter rotating gyre often seen (e.g., in the bottom layer of Fig. 1) in a "four-gyre" structure in the bottom layer of double gyre Q-G eddy resolving models.

Near the southern edge of the domain the surface

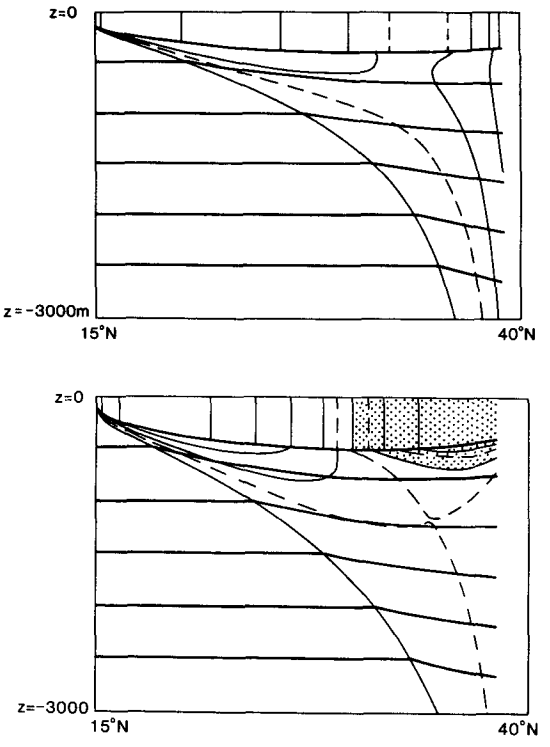

FIG. 13. Meridional cross section across the gyre at (a) 65°W and (b) 80°W. The stratification of Fig. 5 is employed, equivalent to that of Figs. 8–11, but with the addition of a (scaled) buoyancy jump $\Delta B' = 2$ (equivalent to a density jump of 0.8 kg m^{-3}) under the surface layer.

layer thickness returns to its reference value, and the bowl shallows. Given the barotropic westward zonal transport implied by the Ekman pumping, the isopycnals must steepen to a "tulip" shape in a similar manner as at the eastern coast. The shape of the bowl seen in the meridional transect is thus the "champagne glass" seen in the Q-G models; i.e., the "tulip" shaped cup at the south, formed by the wind-driven circulation, merging into the hyperbolic stem associated with the recirculation further north.

We now consider how the broad structure of the flow is modified by variation in the stratification. Suppose that a buoyancy jump between the stratified fluid and the surface layer is introduced. Meridional cross sections of the resulting flow are plotted in Fig. 13, where a "scaled" jump $\Delta B' = 2$ has been chosen; this corresponds to a density jump of 0.8 kg m^{-3}.

This buoyancy jump allows weak shear in the upper layers of the fluid to imply substantial transport in the surface layer; there is thus less need for the isopycnals to steepen at the southern boundary. Also the *zonal* isopycnal slope consonant with a given Sverdrup transport lessens; hence the depression of the surface layer is less marked. Any reversed (i.e., eastward) velocities are likely to be concentrated into the surface layer, as is indeed seen in Fig. 13.

Variation in the *general* strength of the stratification is, of course, proportional to that in the inertial velocity scale U_I. Where the stratification is strengthened, a fixed Ekman pumping is less effective in driving the isopycnals down from their positions on the eastern boundary: it is the ratio U_S/U_I which determines the efficacy of the Ekman pumping. This is consistent with the introduction of the buoyancy jump yielding a greater effective U_I.

The flow fields associated with uniform stratification are displayed in Fig. 14. The slack density gradient of 0.2 kg m^{-3}/km has been supposed, as was used to plot Fig. 5 where it gave reasonable values for the recirculation velocities near the axis of the stream. Again, the ratio $U_S/U_I = 1$. Clearly the gross underestimate of the stratification, particularly near the surface, implies exaggerated distortion of the isopycnals by the wind stress curl. A more realistic picture is generated by decreasing the ratio U_S/U_I to 0.2, as in Fig. 15a; if this is considered as steepening of the stratification to 1 kg m^{-3}/km it must be remembered that the velocity scale U_I has also been multiplied by five. Velocities in the recirculation are then too large. It is apparent that there are major difficulties in choosing a value of the stratification consistent with realistic behavior both in the southern part of the gyre, where the flow is limited to the highly stratified upper waters, and in the northern part of the gyre where the flow extends through the deeper, less stratified fluid.

These difficulties are eased if a buoyancy jump is introduced between the stratified and surface waters. In Fig. 15b, the same stratification as in Fig. 14, 0.2 kg m^{-3}/km is supposed in the stratified fluid, together with a scaled $\Delta B' = 2$ (equal to a density jump of 0.8 kg m^{-3}—the entire buoyancy difference between −4000 m and the surface in Fig. 15a). This is a much better representation of the hyperbolic stratification and the results show much better agreement.

4. Conclusions

The recirculating flow on the southern flank of a separated boundary current—corresponding to, say,

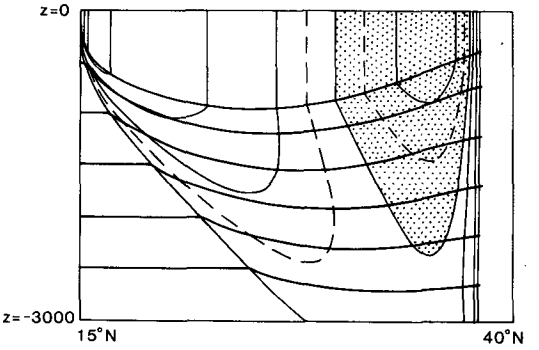

FIG. 14. Meridional cross section across the gyre at 80°W. Uniform stratification as in Fig. 6 is supposed, with a density gradient of 0.2 kg m^{-3} km^{-1}, and no buoyancy jump under the surface layer.

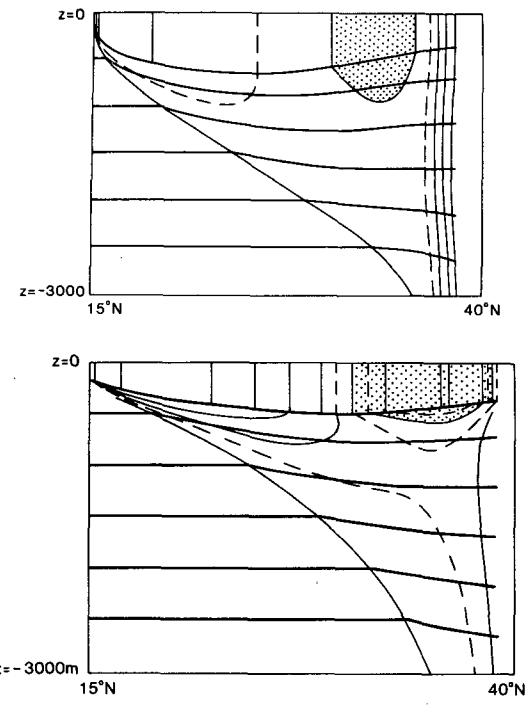

FIG. 15. Meridional cross section across the gyre at 80°W. In (a) uniform stratification is supposed as in Fig. 14 with, however, $U_S/U_I = 0.2$. This may be interpreted as a density gradient 1 kg m^{-3} km^{-1}, in which case velocities are scaled in terms of a $U_I = 7.2$ cm s^{-1}. There is no buoyancy jump under the surface layer. In (b) we suppose a scaled jump in buoyancy $\Delta B' = 2$ (equivalent to a density jump of 0.8 kg m^{-3}), but retain $U_S/U_I = 1$ as in Fig. 14.

the westerly flow between about 80° and 50°W in the north Atlantic—has been discussed in terms of a baroclinic Fofonoff gyre distorted by the application of Ekman pumping. The resulting flow is confined to a surface homogeneous layer and to a bowl of stratified fluid underneath.

One may suppose that potential vorticity in the unventilated stratified fluid below, where it is in motion, takes on the reference value appropriate to fluid at rest underneath the separated jet. Given plausible hypotheses for the depression of the surface mode waters, this leads to the conclusion that this bowl of moving fluid is likely to strike the ocean floor. Where it does so, a barotropic circulation can be driven. The assumption that the potential vorticity of the gyre takes on this value is clearly valid in the Q-G eddy resolving models but less evident in the real ocean. Small variations in the value of the homogenized potential vorticity can make a great difference to the depth of the bowl. In fact, the observations seem to show that the bowl does strike the bottom in the Atlantic, but that it perhaps does not in the Pacific.

The presence of Ekman pumping affects the westward return flow variously. A nonzero depth-integrated meridional mass transport is now set by the anticyclonic wind-stress curl. The flow is thus pulled southward and the latitudinal variation of the wind-stress curl necessitates the development of a corresponding component of zonal flow; i.e., eastward to the north of the line of maximum Ekman pumping, westward to the south of this line. In the southern part of the gyre, this westward flow reinforces and indeed, close to the southern edge, dominates the westward flow fed in from the eastern boundary. To the north, the eastward flow is mostly dominated by the westward recirculation, but may become strong enough near the western edge to reverse the recirculating flow in the upper layers. Anticyclonic shear develops around the western edge of the line of maximum Ekman pumping in the upper stratified layers. This may tentatively be identified with the southern lobe of the "C" seen in corresponding regions of the oceans in maps of the dynamic topography.

Isopycnals and hence the depth of penetration of the bowl of moving fluid deepen towards the west. More interestingly the bowl is forced to take on a tulip shape near the southern boundary associated with the wind driven Sverdrup component of the flow. This represents the cup (the hyperbolic dive associated with the recirculation represents the stem) of the champagne glass-shaped bowl seen in the Q-G models.

These results are relevant as they stand to the Q-G eddy resolving models. Detailed comparison with observations is more difficult, but there is a rough correspondence in the features seen.

Acknowledgments. Much is due to the helpful comments and sustained enthusiasm of John Marshall. This work was done under a research grant from the National Environmental Research Council of the United Kingdom.

REFERENCES

Bower, A. S., H. T. Rossby and J. L. Lillibridge, 1985: The Gulf Stream—Barrier or blender? *J. Phys. Oceanogr.* **15,** 24–32.

Fofonoff, N. P., 1962: Dynamics of ocean currents. *The Sea: Ideas and Observations on Progress in the Study of the Seas,* Vol. I: *Physical Oceanography,* M. N. Hill, Ed., Wiley Interscience, 323–395.

Gill, A. E., 1984: On the behavior of internal waves in the wakes of storms. *J. Phys. Oceanogr.* **14,** 1129–1151.

Hogg, N. G., 1983: A note on the deep circulation of the western North Atlantic: its nature and causes. *Deep-Sea Res.,* **30,** 945–961.

——, R. S. Pickart, R. M. Hendry and W. J. Smethe, Jr., 1986: The northern recirculation gyre of the Gulf Stream. *Deep-Sea Res.,* **33,** 1139–1165.

Holland, W. R., T. Keffer and P. B. Rhines, 1984: Dynamics of the oceanic general circulation: the potential vorticity field. *Nature* **308,** 698–705.

Leetmaa, A. P., and A. F. Bunker, 1978: Updated charts of the mean annual wind stress, convergence in the Ekman layers, and Sverdrup transports in the North Atlantic. *J. Mar. Res.,* **36,** 311–322.

Marshall, J. C., 1984: Eddy mean flow interaction in a barotropic ocean model. *Quart J. Roy. Meteor. Soc.* **110,** 573–590.

——, and A. J. G. Nurser, 1986: Steady, free circulation in a stratified quasi-geostrophic ocean. *J. Phys. Oceanogr.* **16,** 1799–1813.

——, and ——, 1987: Anticyclogenesis and the dynamics of the subtropical circulation. *Quart. J. Roy. Meteor. Soc.*, in press.

Masuzawa, J., 1969: Subtropical mode waters. *Deep-Sea Res.*, **16,** 463–472.

McCartney, M. S., 1982: The subtropical recirculation of mode waters. *J. Mar. Res.*, **40**(Suppl.), 427–464.

McDowell, S., P. B. Rhines and T. Keffer, 1982: North Atlantic potential vorticity and its relation to the general circulation. *J. Phys. Oceanogr.* **12,** 1417–1436.

Munk, W. H., 1950: On the wind driven ocean circulation. *J. Meteor.* **7,** 79–93.

Niiler, P. P., W. J. Schmitz and D-K Lee, 1985: Geostrophic volume transport in high eddy energy areas of the Kuroshio Extension and Gulf Stream. *J. Phys. Oceanogr.*, **15,** 825–843.

Pedlosky, J., and W. R. Young, 1983: Ventilation, potential vorticity homogenization, and the structure of the ocean circulation. *J. Phys. Oceanogr.*, **13,** 2020–2037.

Reid, J. L., 1981: On the Mid Depth Circulation of the World Ocean. *Evolution of Physical Oceanography,* B. A. Warren and C. Wunsch Eds., MIT Press, pp. 70–111.

Rhines, P. B., and W. R. Young, 1982a: A theory of the wind driven circulation I. Mid-Ocean Gyres. *J. Mar. Res.*, **40**(Suppl.), 559–596.

——, and ——, 1982b: Homogenization of potential vorticity in planetary gyres. *J. Fluid Mech.*, **122,** 347–367.

Richardson, P. L., 1985: Average velocity and transport of the Gulf Stream near 55 W. *J. Mar. Res.*, **43,** 83–111.

Schmitz, W. J., 1980: Weekly depth-dependent segments of the North Atlantic circulation. *J. Mar. Res.*, **38,** 111–135.

Stommel, H., 1948: The westward intensification of wind driven ocean currents. *Trans. Amer. Geophys. Union,* **99,** 202–206.

——, and F. Schott, 1977: The beta spiral and the determination of the absolute velocity field from hydrographic station data. *Deep-Sea Res.*, **24,** 325–329.

——, P. P. Niiler and D. Anati, 1978: Dynamic topography and recirculation of the North Atlantic. *J. Mar. Res.*, **36,** 449–468.

Veronis, G., 1966: Wind-driven ocean circulation—Part I. Linear theory and perturbation analysis. *Deep-Sea Res.*, **13,** 17–29.

Worthington, L. V., 1976: On the North Atlantic circulation. *Johns Hopkins Oceanographic Studies,* Vol. VI. The Johns Hopkins University Press, 110 pp.

Wunsch, C., and D. Roemmich, 1985: Is the North Atlantic in Sverdrup balance? *J. Phys. Oceanogr.*, **15,** 1876–1880.